https://doi.org/10.46344/JBINO.2021.v10i06.10

HIV-1 PROTEASE INHIBITION BY TERPENES AND STEROLS COMPOUNDS: IN-SILICO STUDIES

Resmi Mustarichie[1*], Sandra Megantara[1]

[1]Deparment of Pharmaceutical Analysis and Medicinal Chemistry, Faculty of Pharmacy, Padjadjaran University.

Email: resmi.mustarichie@unpad.ac.id

ABSTRACT

HIV is a major source of public health problems globally and has claimed an estimated 33 million people. There are more than 20 compounds of the terpenes and sterols that are useful as anti-HIV agents that can be studied to see if they are bound to the HIV-1 receptor compounds. In this article, we will discuss the in silico 20 terpenes and sterols approach to the HIV-1 receptor. And the result is that the compound has a better free energy binding value than lamivudine as a drug standard and may be used for HIV-1 treatment.

Keywords: Anti HIV-1, sterols, terpenes, in silico

Introduction

HIV is a major source of public health problems globally and has claimed an estimated 33 million people (WHO, 2021). Human Immunodeficiency Virus (HIV) attacks the immune system and weakens the body's defenses against various infections and cancers. As the virus destroys and destroys immunity, the infected body gradually sheds immunity as measured by looking at CD4 cells. After HIV infects the immune system. Furthermore, it will cause progressive damage to the immune system that continues in Acquired immunodeficiency syndrome (AIDS) (Yaseen, 2017). There is no cure for HIV infection. However, HIV can be controlled and prevented by antiretroviral drugs. Despite the presence of antiretrovirals, HIV / AIDS has now become the leading cause of death in Sub-Saharan Africa while ranking fourth in the world. In 2018, out of 37.9 million people suffering from HIV, 3.8 million of them lived in Southeast Asian countries (WHO, 2021).From here, it is necessary to develop drugs that can cure an infection of HIV. In this article, the authors report an approach related to compounds that can inhibit the HIV-1 virus which can be used as a reference for further research. The article that discusses natural products that have anti-HIV activity shows various active compounds that act as anti-HIV. One of them is in the terpenes and sterols (Sillapachaiyaporn and Chuchawankul, 2019). There are more than 20 compounds that are useful as anti-HIV drugs that can be studied to see the binding with the HIV-1 receptor compound.

Materials and Methods

Molecular Docking

Molecular docking studies were carried out using AutoDock 4.0 software. The crystal structure of the HIV-1 PR X-ray (PDB ID: 5KR0) (Liu et.al, 2016) was downloaded from the RCSB Protein Data Bank. Target proteins were made by removing ligands and water molecules and adding the missing hydrogen. All ligands were downloaded from PubChem and prepared using AutoDock. In the grid-based approach used in this study, the position of the grid boxes was arranged following the original inhibitor of the protein (glycerol for HIV-1 PR). For HIV-1 PR, the grid size was set to 40 x 40 x 40 XYZ points with a grid spacing of 0.375 Å in the center of the protein. The XYZ centers of the grid squares were at -16,847, 12,525, -19,777, respectively. Docking simulations were performed using the Lamarck genetic algorithm with default parameters. DG) was selected to further study protein-ligand interactions using the Discovery studio visualizer. The results were compared with the original ligands of these receptors.

Pre-ADMET

ADMET parameters were identified using the preADMET® program which can be accessed through the website http://preadmet.bmdrc.kr/adme/ (preAdmet, 2020). The chemical structure of the compounds from Pubchem was converted into Mol (* .mol) file format. The program automatically calculated the predictive value of selected parameters, including the permeability of human colon adenocarcinoma cells (Caco-2), Human Intestinal Absorption (HIA), Plasma Protein Binding (PPB), the toxicity of compounds including mutagenic and carcinogenic

Results and Discussion

In this study, the 5KR0 protein receptor shown in Figure 1 was used to see the activity of sterols and terpenes as anti-HIV-1 in silico whereas in previous studies this receptor was also used for anti-HIV-1 testing in extracts (*Lignosus rhinocerus*).

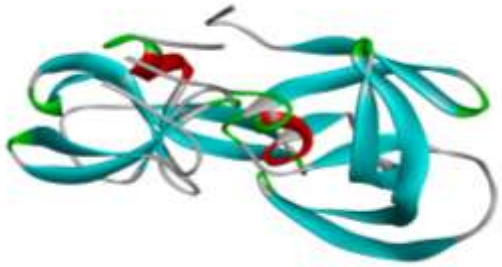

Figure 1. 5KR0 protein

When preparing the 5KR0 protein, AutoDock Tools 4.2 software was used to determine the grid box in the area used as the active site of the protein to bind with ligands. Determining the grid box includes setting the location of the parameter box and determining the size of the grid box using the distance (angstrom). In this 5KR0 protein, the results obtained from the grid box were center x = -16,847; y = 12.525 and z = -19.777 with a grid point distance (Angstrom) of 0.375 Å (Figure 2).

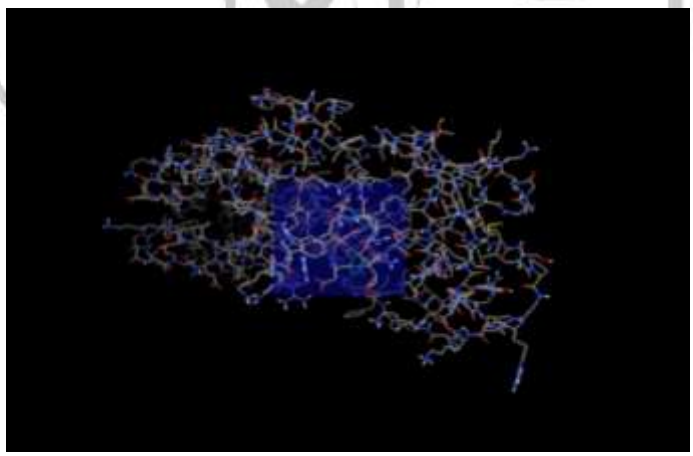

Figure 2.Protein preparation with autodock 4.2

For the manufacture of ligands, the components of the sterol and terpenes groups used the drug ratio, namely {3 - [(4-amino-benzenesulfonyl) -isobutyl-amino] -1-benyl-2-hydroxy-propyl} -carbamic acid tetrahydrofuran-3-yl ester.

Compounds studied is listed in Table 1.

Table 1. Component of compounds on the comparative drug, native ligand, and test compounds

Compounds	Molecular Formula	Structure

1β-hydroxymaprounic acid 3-p-Hydroxybenzoate	C37H52O6	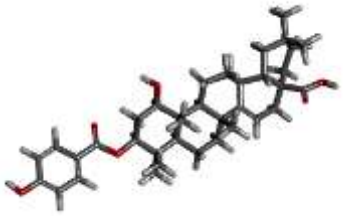
12-Deoxyphorbol-13- (3E, 5E-decadienoate)	C30H42O6	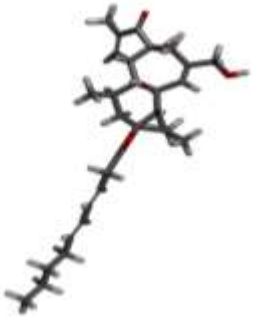
Artemisinin	C15H22O5	
Betulinic acid	C30H48O3	
Celasdin B	C30H50O3	
Clausenolide-1-ethyl ether	C27H36O8	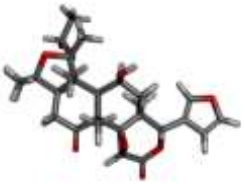

Cyanthiwigin B	C20H28O2	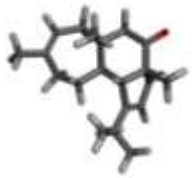
Dihydrobetulinic acid	C30H50O3	
Haplosamates B	C29H51NO14S3	
Lancilactone C	C30H40O4	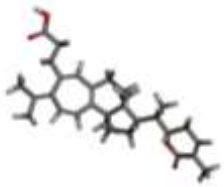
Limonene	C26H30O8	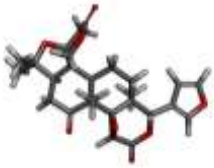
Linearol	C22H34O4	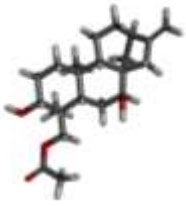

Maslinic acid C30H48O4

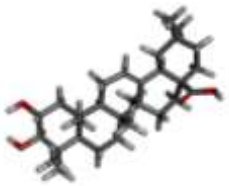

Moronic acid C30H46O3

Oleanolic acid C30H48O3

Nomilin C28H34O9

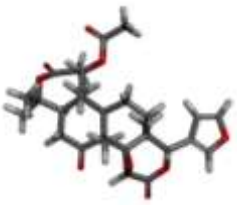

.

Prostratin C22H30O6

Suberosol C31H50O2

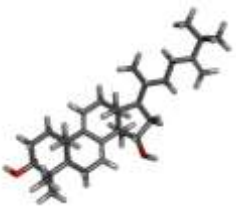

Ursolic acid	C30H48O3	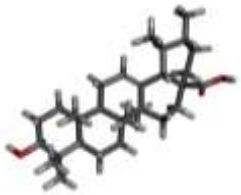
Uvaol	C30H50O2	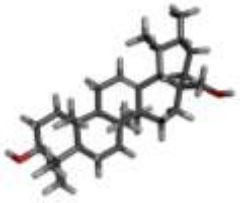

Method Validation

In this study, the analysis used to evaluate the validation results were to look at the RMSD value and the binding location. The parameter used was considered valid if the RMSD value obtained was ≤ 2.00 Å. In this study, the validation results obtained for the RMSD value of 1.503 A, indicated that it met the requirements so that these parameters could be used to simulate the docking of test compounds and comparison drugs.

Docking Interaction of Test and Visualization Compounds

In this study, 21 compounds of the sterols and terpenes found in natural ingredients and drugs as a comparison was carried out by tethering or docking with the receptors using Autodock Tools 4.2 software with a grid box dimension of 40 × 40 × 40. amino acid residues indicating binding to the active site of the HIV-1 receptor. Also, the free energy bond (ΔG) and the inhibitory constant (Ki) was obtained, as shown in Table 2.

Table 2. Molecular results of docking candidate ligands against active HIV-1 PR sites.

Compound	**Interactions with Amino Acid Residues**		**Ki**	**(ΔG)**
	Hydrogen Bonds	**Van der Waals (hydrofobic)**		
Lamivudine	Conventional hydrogen bond (ASN 25; ASP 30) Carbon hydrogen bond (GLY 27)	LEU 76; ASP 29; VAL 32; GLY 27; ALA 28; GLY 49; ILE 84; ASN 25	345.65 uM	-4.75 Kcal / mol

1beta-hydroxymaprounic acid 3-p-hydroxybenzoate	Conventional hydrogen bond (ASP 30; GLY 48)	LEU 76; LEU 23; LEU 47; ILE 47; ILE84; ARG 8; GLY 49; GLY 27; ASP 29; PRO 81	747.09 pM	-12.45 Kcal / mol
12-Deoxyphorbol-13- (3E, 5E-decadienoate)	Conventional hydrogen bond (ASN 25; ASP 30; ASP 29; ARG 8; GLY 27; GLY 48) Carbon hydrogen bond (ASP 30)	PRO 81; GLY 49; ILE 50; ILE 84; GLY 27; GLY 48; ILE 47; ASP 30; LEU 76; ASP 29; THR 31; ALA 28	9.81 nM	-10.93 Kcal / mol
Artemisinin	Conventional hydrogen bond (ILE 50; THR 80) Carbon hydrogen bond (PRO 81)	ASN 25; GLY 27; GLY 48; GLY 49; LEU 23; ALA 28	1.27 uM	-8.04 Kcal / mol
Betulinic acid	Conventional hydrogen bond (GLY 48; ASP 30) Carbon hydrogen bond (GLY 49)	GLY 48; GLY 27; ILE 47; GLY 49; ILE 50; ILE 84; AASN 25; ASP 29; LEU 76	1.99 nM	-11.87 Kcal / mol
Celasdin B	Conventional hydrogen bond (GLY 27; VAL 82)	GLY 48; GLY 49; LEU 23; ILE 84; PRO 81; GLY 27; ASP 29; ALA 28; ASN 25; ILE 50; VAL 32; ASP 30; LEU 76	6.20 Nm	-11.20 Kcal / mol
Clausenolide-1-ethyl ether	Conventional hydrogen bond (ASN 25; ASP 29) Carbon hydrogen bond (GLY 49; ASP 29)	GLY 27; PRO 81; VAL 82; THR 80; ASN 25; GLY 49; ASP 30; GLY 48; LEU 23; ILE 47	22.84 Nm	-10.42 Kcal / mol
Cyanthiwigin B	Conventional hydrogen bond (ASN 25)	ILE 84; GLY 27; GLY 49; ASN 25; ILE 50; VAL 32; ASP 30; ASP 29; GLY 48	296.59 nM	-8.91 Kcal / mol
Dihydrobetulinic acid	Conventional hydrogen bond (GLY 48; ASP 30) Conventional hydrogen bond (GLY 49)	LEU 76; ASP 29; GLY 49; GLY 48; GLY 29; GLY 27; ASN 25; ILE 84; ILE 50; ILE 47	1.37 nM	-12.09 Kcal / mol

Diterpenoid SP-II	Conventional hydrogen bond (ASP 29; ASP 30; ASN 25)	ILE 84; ALA 28; GLY 49; GLY 27; VAL 32; LEU 76; GLY 48	176.91 nM	-9.21 Kcal / mol
Haplosamates B	Conventional hydrogen bond (GLY 48; GLY 27) Carbon hydrogen bond (GLY 27; GLY48; THR 80)	ASP 29; LEU 23; GLY 49; VAL 82; PRO 81; ILE 84; ILE 50; ASN 25; ALA 28; PHE 53; ILE 47	195.20 nM	-9.15 Kcal / mol
Lancilactone C	Conventional hydrogen bond (ASP 49; ASP 50)	ASN 25; LEU 23; GLY 27; GLY 48; GLY 49; ILE 50; ILE 84; PRO 81; VAL 82; ILE 47	5.29 nM	-11.29 Kcal / mol
Limonine	Conventional hydrogen bond (ASN 25) Carbon hydrogen bond (ASP 30)	GLY 48; GLY 49; ILE 84; VAL 82; GLY 27; LEU 23; LEU 76; ASP 29; PRO 81; ASN 25; ILE 47	25.70 uM	-10.29 Kcal / mol
Linearol	Conventional hydrogen bond (ARG 8)	ASP 30; ASP 29; GLY 48; LEU 23; VAL 82; GLY 27; ILE 84; ASN 25; GLY 49	183.64 Nm	-9.19 Kcal / mol
Maslinic acid	Conventional hydrogen bond (ASP 30; ARG 48; ILE 50)	LEU 76; GLY 48; GLY 27; GLY 49; ASN 25; ILE 84; ASP 29	1.26 nM	-12.14 Kcal / mol
Moronic acid	Conventional hydrogen bond (ASP 29; ASP 30; GLY 48) Carbon hydrogen bond (GLY 49)	GLY 48; VAL 32; GLY 27; ILE 47; ILE 50; ASP 29; ILE 84; ASN 25; GLY 49	3.75 nm	-11.49 Kcal / mol
Oleanolic acid	Conventional hydrogen bond (ILE 50; ASP 30; GLY 48)	GLY 27; GLY 49; ASN 25; ILE 84; ASP 29; GLY 48	3.09 Nm	-11.61 Kcal / mol
Nomilin	Conventional hydrogen bond (ASP 29)	VAL 82; PRO 81; ILE 84; LEU 23; ASN 25; GLY 27; ASP 30; GLY	66.21 Nm	-9.79 Kcal / mol

	Carbon hydrogen bond (GLY 27; GLY 49)	49; GLY 48; ASP 29		
Prostratin	Conventional hydrogen bond (GLY 48; GLY 27; ARG 8; ASP 29; ASP 30; ILE 50)	ASN 25; ALA 28; ILE 47	29.94 Nm	-10.26 Kcal / mol
	Carbon hydrogen bond (GLY 49)			
Suberosol	Conventional hydrogen bond (ASP 30)	LEU 76; VAL 32; ILE 84; ASN 25; GLY 49; GLY 48; ASP 30; ASP 29; PRO 81; VAL 82; GLY 27	2.26 nM	-11.80 Kcal / mol
	Conventional hydrogen bond (ASP 30; GLY 49)	LEU 76; ASP 29; GLY 48; GLY 27; GLY 49; ASN 25; ILE 84	2.52 Nm	-11.73 Kcal / mol
Ursolic acid	Carbon hydrogen bond (GLY 49)			
Uvaol	Conventional hydrogen bond (ASP 30; GLY 48)	LEU 76; ASP 29; GLY 48; GLY 27; GLY 49; ASN 25; ILE 84; ILE 47;	1.31 Nm	-12.12 Kcal / mol

Table 2 showed the value of the free energy bond (ΔG) and the inhibitory constant (Ki). A comparison of the free-energy bonds between the candidate ligands and the original ligands. In theory, a low free-energy bond indicates a good predictor of molecular docking. For HIV-1 PR analysis (PDB ID: 5KR0) with docking determination, low bond energy of lamivudine as a standard drug with HIV-1 PR was -4.75 kcal/mol and a KI value of 345.65 uM. For all candidate compounds listed in table 2, there was no BE value ≥ -4.75 kcal/mol. From this low BE value, it could be said that the docking prediction was good. The receptor-ligand interactions suggest that all candidate ligands might be inserted into the HIV-1 PR binding pocket similar to lamivudine and were predictable anti-HIV-1 candidates.

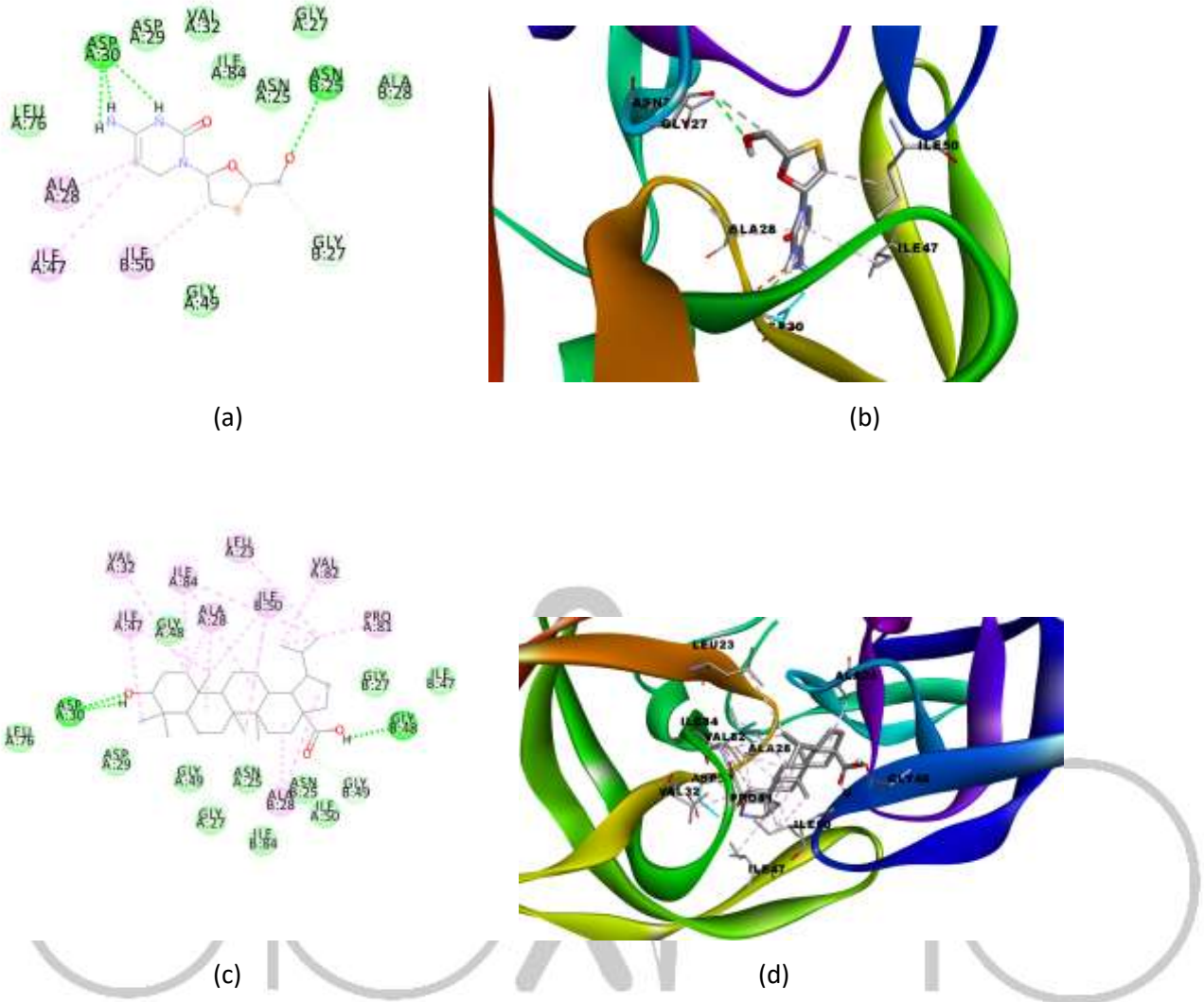

Figure 3. Docking result visualization from lamivudine of 2D (3.a) and 3D (3.b); Dihydrobetulinic acid of 2D (3.c) and 3D (3.d)

Pre-ADMET

New drug candidates must pay attention to pharmacokinetic parameters including absorption, distribution, and toxicity to obtain results consistent with clinical trials. Parameters for pharmacokinetic properties consist of absorption [(HIA) and Caco-2] and distribution (PPB), for toxicity seen from mutagenic and carcinogenic properties. Where HIA was the value of bioavailability and absorption of the ratio of excretion or cumulative excretion in urine, bile, and feces, while Caco-2 was used as an in-vitro model in predicting drug absorption in humans. Distribution parameters used PPB because it was closely related to drug disposition in giving effect (Megantara et.al, 2018). The pre-ADMET results can be seen in table 3.

Table 3 Pre-ADMET prediction results

Compound	Absorption		Distribution		
	HIA (%)	Caco-2 (nm sec-1)	PPB (%)	Mutagenic	Carcinogenic
1beta-hydroxymaprounic acid 3-p-hydroxybenzoate	95.376444	21,5123	99.45747	Positive	Positive
12-Deoxyphorbol-13- (3E, 5E-decadienoate)	92.402923	20.9632	91,886201	Negative	Positive
Artemisinin	96.314307	30.3276	93,368123	Positive	Negative
Betulinic acid	95.996396	21.8616	100	Positive	Negative
Celasdin B	94.183553	22,861	100	Negative	Negative
Clausenolide-1-ethyl ether	95.233669	37,1656	64,716698	Negative	Negative
Cyanthiwigin B	99,11582	31,0496	100	Positive	Positive
Dihydrobetulinic acid	95.94531	21,8836	100	Negative	Negative
Diterpenoid SP-II	90.492737	17.6869	93.623685	Negative	Negative
Haplosamates B	41.468316	5,3663	81.803752	Negative	Positive
Lancilactone C	97.63901	23.8627	96.091584	Negative	Positive
Limonine	96.259564	27.6795	80.276857	Negative	Negative
Linearol	92.837139	21,5877	88.276846	Positive	Negative
Maslinic acid	94,27737	21.28	100	Negative	Positive
Moronic acid	97.629839	22,2701	100	Negative	Positive
Oleanolic acid	95.996305	21,8872	100	Negative	Positive
Nomilin	94.205765	25,2719	83.163053	Negative	Negative
Prostratin	87.326232	18,0219	62.962894	Negative	Positive
Suberosol	94,785983	36.8468	97.529563	Positive	Positive
Ursolic acid	95.996396	21.8616	100	Negative	Positive
Uvaol	94.405824	24,6579	100	Negative	Positive

Based on the literature, the range of% HIA absorption values of 70 - 100% indicated that the drug was well absorbed, 20 - 70% indicated that the drug was moderately absorbed and 0 - 20% indicates that the drug was poorly absorbed. For Caco-2 (nm sec-1) in vitro, the cell permeability value> 70 nm sec-1 indicated higher permeability, 40-70 nm sec-1 indicates moderate permeability and <4 nm sec-1 indicates low permeability. (Nursamsiar, 2016)

The results of the Pre-ADMET in Table 3. show the absorption rate of% HIA with a range of values close to 100% in all compounds, which means that the compounds identified can be absorbed very well in the intestine while Caco-2 ranges from 5 - 37 nm sec-1 which indicates a moderate permeability value. when there is the transport of the drug through the intestinal epithelium of adenocarcinoma in the human colon. The distribution parameter is based on the value of plasma protein bonds, indicating that almost all compounds have PPB close to 100%. This suggests that diffusion occurs through the plasma membrane and interacts with pharmacological targets (Nursamsia et.al, 2016). Human plasma contains 70% protein with albumin (Human Serum Albumin, HAS), a 1-glycoprotein (AGP), and lipoprotein as its main components (Megantara et.al, 2018). While the result of toxicity, all compounds are hardly mutagenic but are carcinogenic.

Conclusion

The results of screening for terpenes and sterols listed in table 2 using the in silico method showed better activity against HIV-1 than lamivudine as a comparative drug. The absorption value of intestinal permeability and Caco-2 cells showed very good results. For the distribution based on the value of plasma protein bonds, it was estimated that it could diffuse through the plasma membrane and interact with pharmacological targets and the toxicity results of several compounds indicated no mutagenic and carcinogenic risks. So it concluded that the Celasdin B compound, Clausenolide-1-ethyl ether, Dihydrobetulinic acid, Diterpenoid SP-II, Limonin, and Nomilin could be used as HIV-1 drug candidates because they had better ΔG values and were not carcinogenic and mutagenic.

References

WHO - Organisasi Kesehatan Dunia. (2021). https://www.who.int/hiv/data/en/ [download on January 2021]

Yaseen, M.M., Abuharfeil, N.M., Alqudah, M.A. (2017). Mechanisms and factors that drive extensive human immunodeficiency virus type-1 hypervariability: an overview, Viral Immunol. 30 (10):708.

Sillapachaiyaporn, C. and Chuchawankul, S.(2019). HIV-1 protease and reverse transcriptase inhibition by tiger milk mushroom (Lignosus rhinocerus) sclerotium extracts: In vitro and in-silico studies. Journal of Traditional and Complementary Medicine. doi:10.1016/j.jtcme.2019.08.002

Liu Z, Huang X, Hu L, et al. (2016). Effects of hinge Region natural polymorphisms on human immunodeficiency virus-1 protease

structure, dynamics, and drug pressure evolution. J Biol Chem. 291(43):22741e22756.
pre-ADMET. Available from: http://preadmet.bmdrc.kr/adme/. (Downloaded on December 15, 2020).

Megantara, S., Levita, J., Iwo, M.I., Ibrahim, S. (2018). Absorption, distribution and toxicity prediction of andrographolide and its derivatives as anti-HIV drugs. Res J Chem Environ. 18;22(Special Issue 1):82–5.

Nursamsiar, N., Toding, A.T., Awaludin, A. (2016)Studi In Silico Senyawa Turunan Analog Kalkon dan Pirimidin sebagai Antiinflamasi: Prediksi Absorpsi. Distribusi, dan Toksisitas. Pharmacy. 13(1):92–100.